

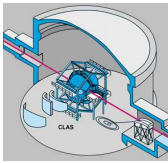
New experimental constraints on the polarizability corrections in the hydrogen hyperfine structure

Keith Griffioen

email: `griff@physics.wm.edu`

Dept. of Physics

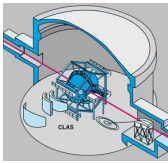
College of William & Mary, Williamsburg, VA



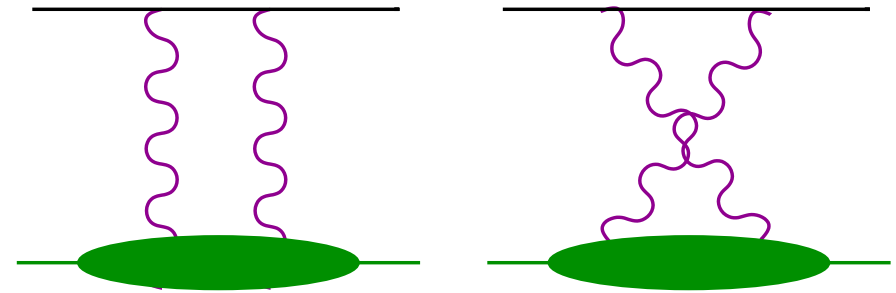
- It has long been known that nuclear structure influences hyperfine splittings in atoms.
- Zemach, [PR104\(56\)1771](#), calculates hfs contribution from proton form factors.
- Drell and Sullivan, [PR154\(67\)1477](#), calculate the polarizability contribution to hydrogen hfs.
- Faustov and Martynenko, [EPJC24\(02\)281](#), estimate polarizability contribution to hydrogen hfs.
- Friar and Sick, [PLB579\(04\)285](#), determine the Zemach radius from world form factor data.
- Brodsky, Carlson, Hiller and Hwang, [PRL94\(05\)022001](#), determine Zemach radius via Faustov.
- The inconsistencies call for an updated determination of the polarizability contribution.



Hyperfine Splitting



- Feynman diagrams for proton polarizability term in the hydrogen hyperfine splitting

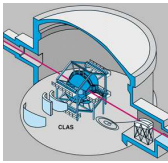


Ground-state hyperfine splittings have been measured to 13-digit accuracy. The largest theoretical uncertainty comes from Δ_S (proton structure).

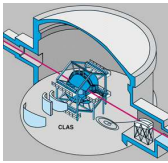
$$E_{\text{HFS}}(e^- p) = 1.4204057517667(9)\text{GHz} = (1 + \Delta_{\text{QED}} + \Delta_R^p + \Delta_S) E_F^p$$

$$E_{\text{HFS}}(e^- \mu^+) = 4.463302765(53)\text{GHz} = (1 + \Delta_{\text{QED}} + \Delta_R^\mu) E_F^\mu$$

in which the Fermi energy $E_F^N = \frac{8}{3} \alpha^4 \mu_N \frac{m_e^2 m_N^2}{(m_N + m_e)^3}$



- Brodsky, Carlson, Hiller, Hwang use hydrogen and muonium to extract an experimental $\Delta_S = -37.66(16)$ ppm.
- $\Delta_S = \Delta_Z + \Delta_{\text{pol}}$
- Zemach: $\Delta_Z = -2\alpha m_e \langle r \rangle_Z (1 + \delta_Z^{\text{rad}})$
- $\langle r \rangle_Z = -\frac{4}{\pi} \int_0^\infty \frac{dQ}{Q^2} \left[G_E(Q^2) \frac{G_M(Q^2)}{1+\kappa} - 1 \right]$
- $\Delta_{\text{pol}} = \frac{\alpha m_e}{2\pi(1+\kappa)M} (\Delta_1 + \Delta_2) = (0.2264798 \text{ ppm})(\Delta_1 + \Delta_2)$
- Friar and Sick: $\langle r \rangle_Z = 1.086 \pm 0.012$ fm from experiment. $\Delta_Z = -41.0(5)$ ppm.
- This all would imply that $\Delta_{\text{pol}} = 3.34(58)$ ppm.
- Faustov and Martynenko obtain $\Delta_{\text{pol}} = 1.4 \pm 0.6$ ppm from a model loosely constrained by SLAC E143 data.

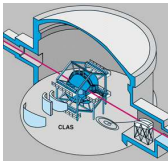


$$\Delta_1 = \int_0^\infty \frac{dQ^2}{Q^2} \left\{ \frac{9}{4} F_2^2(Q^2) - 4M \int_{\nu_{\text{th}}}^\infty \frac{d\nu}{\nu^2} \bar{\beta}_1(\tau) g_1(\nu, Q^2) \right\}$$

$$\Delta_2 = -12M \int_0^\infty \frac{dQ^2}{Q^2} \int_{\nu_{\text{th}}}^\infty \frac{d\nu}{\nu^2} \beta_2(\tau) g_2(\nu, Q^2)$$

in which

- $\nu_{\text{th}} = m_\pi + \frac{m_\pi^2 + Q^2}{2M}$
- $F_2(Q^2)$ is the Pauli form factor
- $\tau = \frac{\nu^2}{Q^2}$
- g_1 and g_2 are the polarized structure functions
- and $\beta_{1,2}$ are kinematic functions



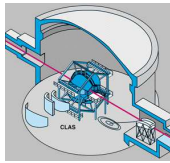
$$\Delta_1 = \frac{9}{4} \int_0^\infty \frac{dQ^2}{Q^2} \left\{ F_2^2(Q^2) + \frac{8M^2}{Q^2} \int_0^{x_{\text{th}}} dx \beta_1(\tau) g_1(x, Q^2) \right\}$$

$$\Delta_2 = -24M^2 \int_0^\infty \frac{dQ^2}{Q^4} \int_0^{x_{\text{th}}} dx \beta_2(\tau) g_2(x, Q^2)$$

- $x_{\text{th}} = \frac{Q^2}{Q^2 + m_\pi^2 + 2Mm_\pi}$
- Advantage: experiments evaluate $\int f(x) g_{1,2} dx$, so error analysis is simplified.
- Disadvantage: large, canceling integrands as $Q^2 \rightarrow 0$.



$\beta_1(\tau)$ **and** $\beta_2(\tau)$



- $\tau = \frac{v^2}{Q^2} = \frac{Q^2}{4M^2x^2}$

- $\beta_1(\tau) =$

- $\frac{4}{9} \left[-3\tau + 2\tau^2 + 2(2 - \tau)\sqrt{\tau(\tau + 1)} \right]$

- $\beta_2(\tau) = 1 + 2\tau - 2\sqrt{\tau(\tau + 1)}$

- $\beta_1(\tau) \rightarrow 0$ as $\tau \rightarrow 0$

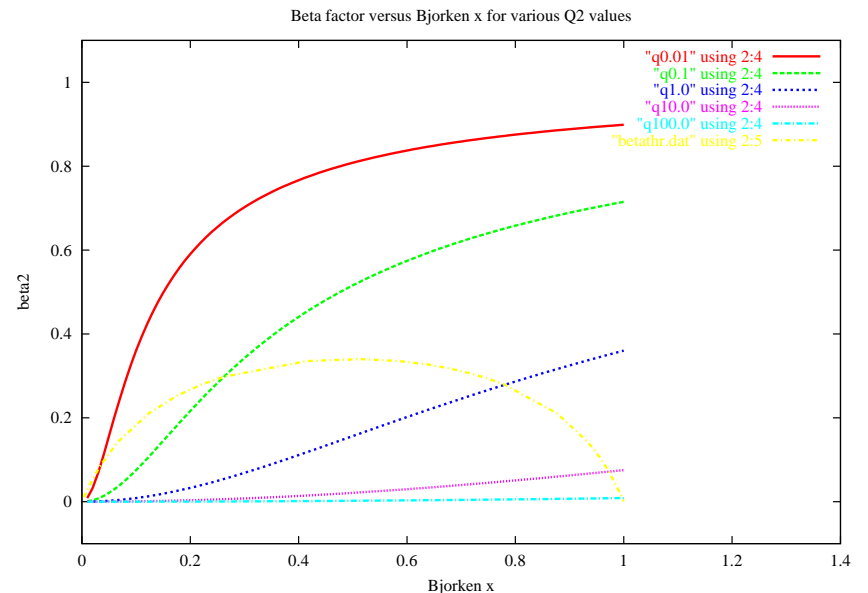
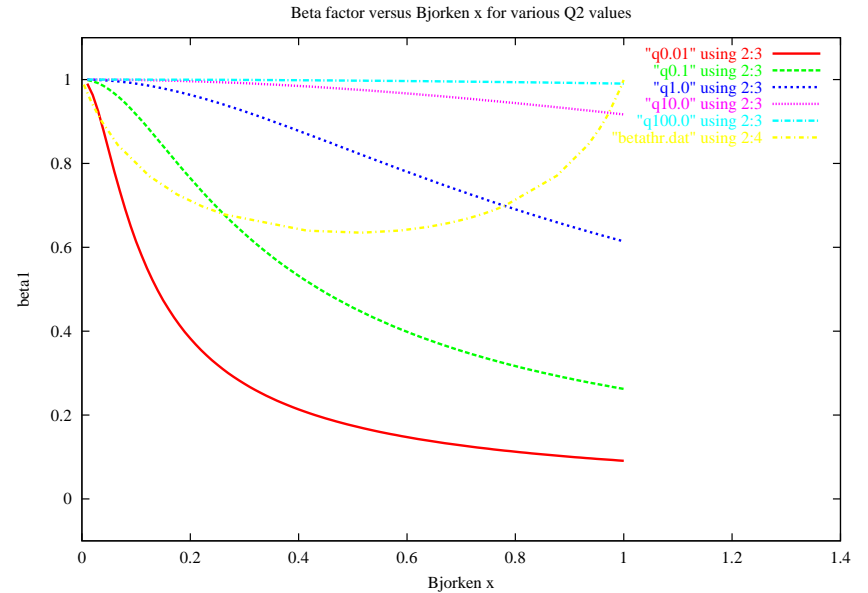
- $\beta_1(\tau) \rightarrow 1$ as $\tau \rightarrow \infty$

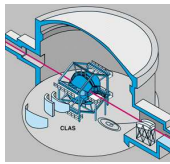
- $\beta_2(\tau) \rightarrow 1$ as $\tau \rightarrow 0$

- $\beta_2(\tau) \rightarrow 1/4\tau$ as $\tau \rightarrow \infty$

- $\int \beta_1 g_1 dx \sim (0.8 - 1.0) \times \Gamma_1$

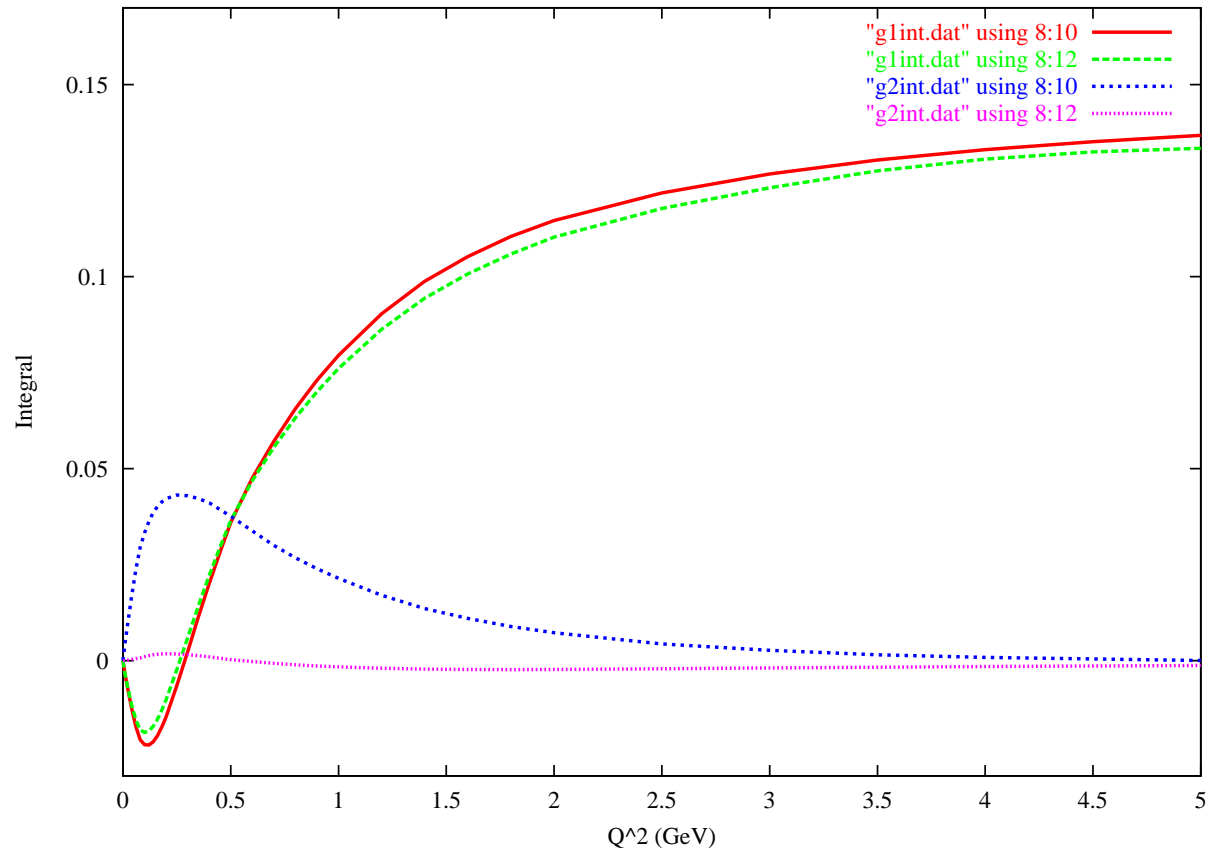
- $\int \beta_2 g_2 dx \sim (0.0 - 0.2) \times \Gamma_2$





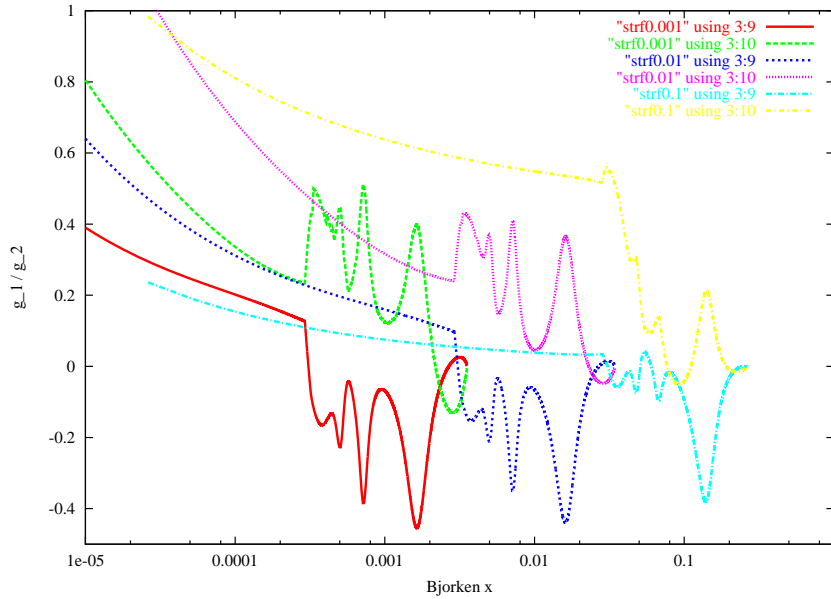
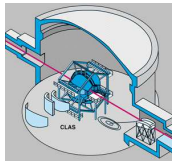
Comparisons between $\Gamma_1 = \int g_1 dx$ and $B_1 = \int \beta_1 g_1 dx$
and between $\Gamma_2 = \int g_2 dx$ and $B_2 = \int \beta_2 g_2 dx$

- $B_1 \approx \Gamma_1$
- $B_2 \approx 0$
- Experimentally, errors on Γ_1 are understood; we exploit this fact.
- $\Gamma_2 = \int g_2 dx \neq 0$ at low Q^2 .

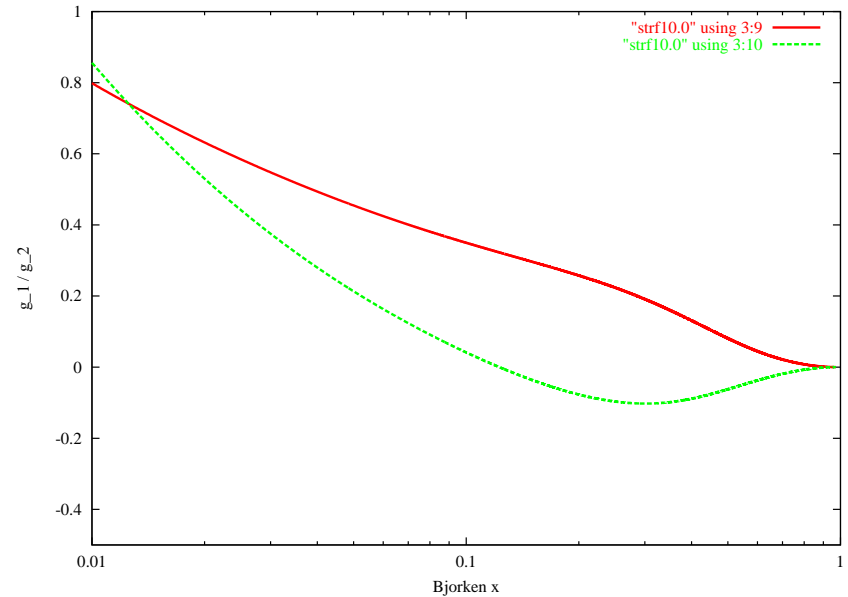
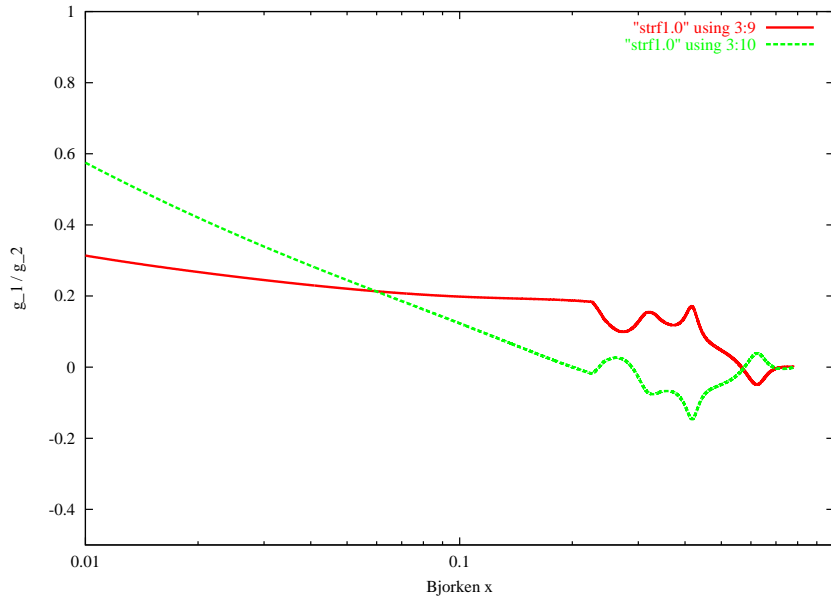




Model g_1 and g_2

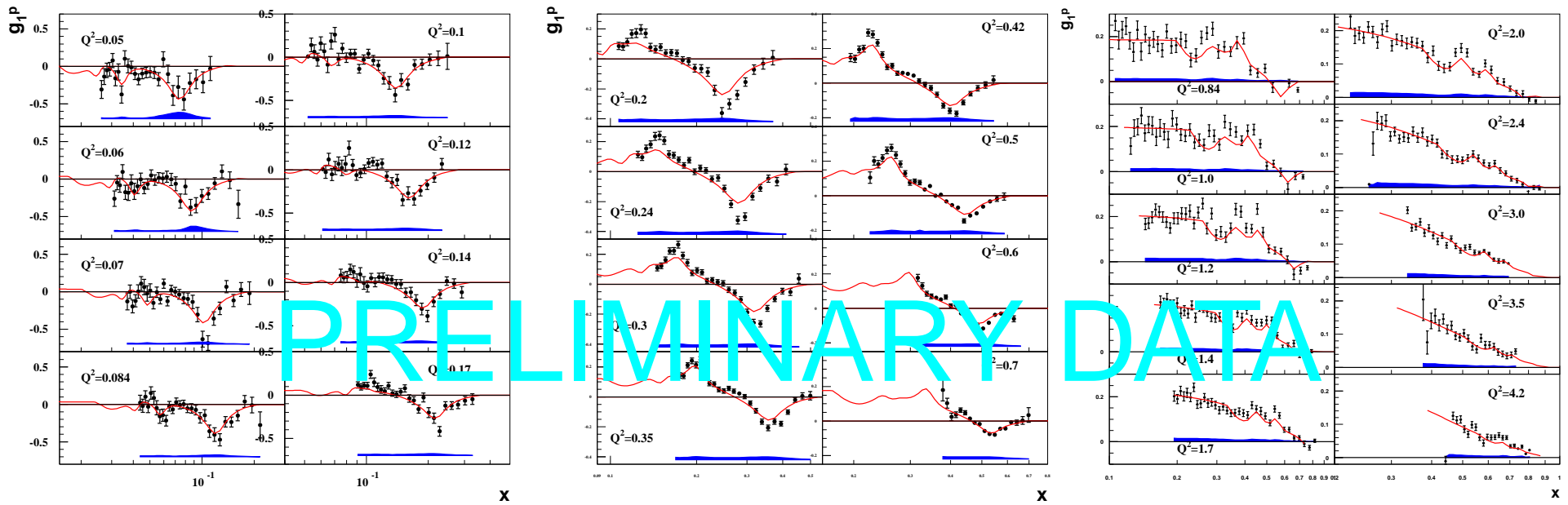
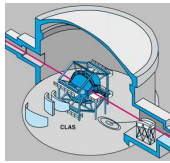


- MAID parameterization in resonance region
- E155 fit in DIS region
- g_2^{WW} in DIS region
- $Q^2 =$
0.001, 0.01, 0.1, 1.0, 10.0

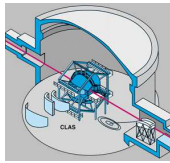




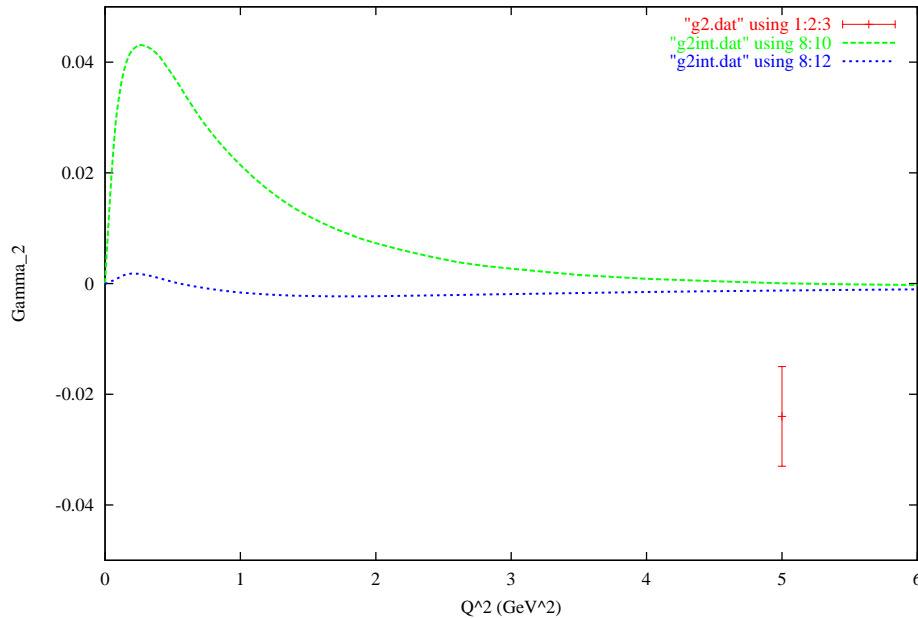
CLAS g_1 with Model



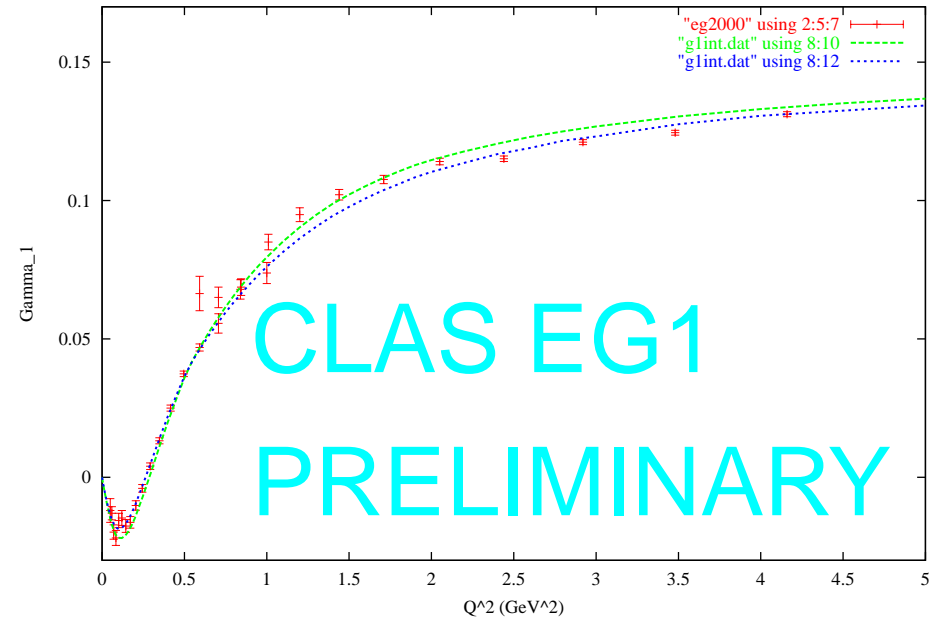
- Preliminary CLAS g_1 data
- $0.05 < Q^2 < 4.2 \text{ GeV}^2$
- **Red line: Model**
- Model reproduces the data quite well over the full range kinematics.



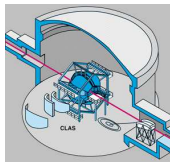
SLAC E155x data with the model



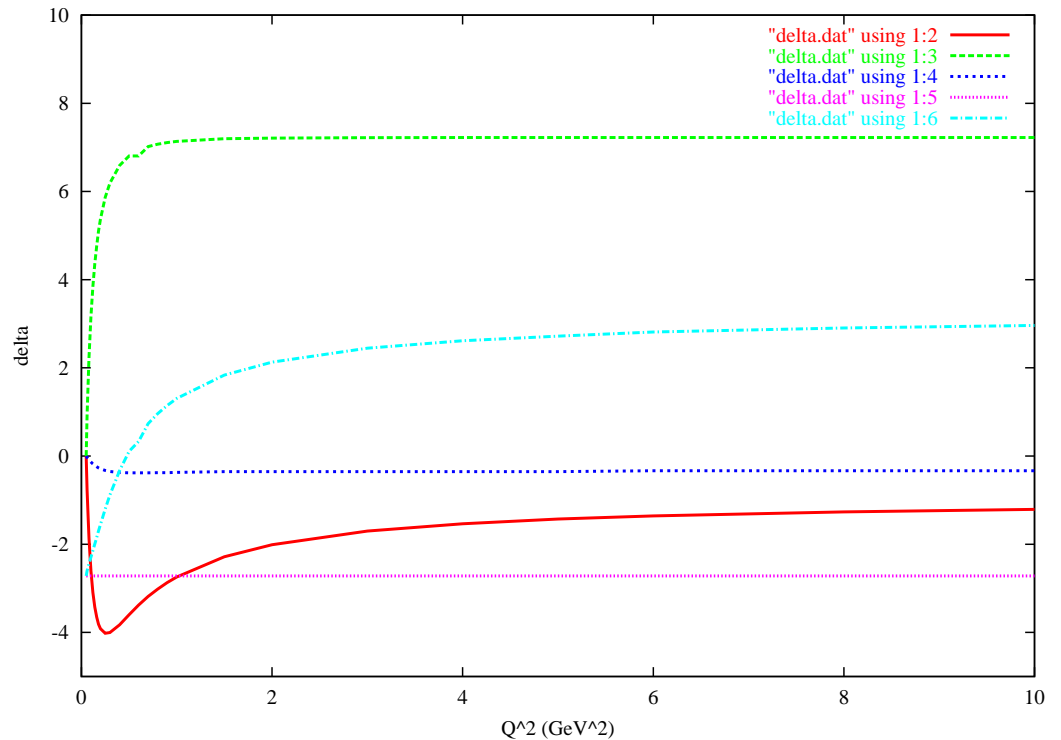
PRELIMINARY eg2000 (CLAS) data with the model

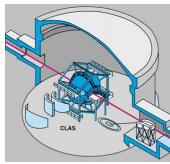


- Left plot: E155x data for $\Gamma_2 = \int g_2(x, Q^2) dx$ with model (green, upper curve) and $B_2 = \int \beta_2 g_2 dx$ (blue, lower curve)
- Right plot: CLAS data for $\Gamma_1 = \int g_1(x, Q^2) dx$ with model (green, upper curve) and $B_1 = \int \beta_1 g_1 dx$ (blue, lower curve)



- Running integrals over Q^2
- Magenta: Δ_{pol} up to $Q^2 = 0.05 \text{ GeV}^2$
- Red: $\Delta_1^{g_1}$ for $[0.05, Q^2]$
- Blue: Δ_2 for $[0.05, Q^2]$
- Green: $\Delta_1^{F_2}$ for $[0.05, Q^2]$
- Cyan: $\Delta_{\text{pol}} = \Delta_1^{g_1} + \Delta_2 + \Delta_1^{F_2}$

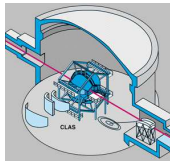




- $G_E = F_1 - \frac{Q^2}{4M^2} F_2$ $G_M = F_1 + F_2$
- $F_2(0) = \kappa$ $F_1(0) = 1$ $G_E(0) = 1$ $G_M(0) = 1 + \kappa$
- $\langle r_E^2 \rangle = -\frac{6}{G_E(0)} \frac{dG_E(Q^2)}{dQ^2} \Big|_0$ $\langle r_M^2 \rangle = -\frac{6}{G_M(0)} \frac{dG_M(Q^2)}{dQ^2} \Big|_0$
- $\frac{dF_2}{dQ^2} \Big|_0 = \frac{dG_M}{dQ^2} \Big|_0 - \frac{dG_E}{dQ^2} \Big|_0 - \frac{\kappa}{4M^2}$
- Friar and Sick:
 $\langle r_E^2 \rangle = (0.895 \pm 0.018 \text{ fm})^2$ $\langle r_M^2 \rangle = (0.855 \pm 0.035 \text{ fm})^2$
- GDH Sum Rule: $\frac{\Gamma_1}{Q^2} = -\frac{\kappa^2}{8M^2}$ as $Q^2 \rightarrow 0$
- $\Delta_1^{[0,0.05]} = \frac{9}{4} \int_0^{0.05} \frac{dQ^2}{Q^2} \left\{ \kappa^2 + 2 \frac{dF_2}{dQ^2} \Big|_0 Q^2 - \kappa^2 \right\}$
- $\kappa = 1.79284739(6)$ $M = 0.938272029(80) \text{ GeV}$
- $\Delta_1^{[0,0.05]} = -2.35 \pm 0.30$ (-2.07) in 2nd order
- Bosted form factor fit: $\Delta_1^{[0,0.05]} = -2.44301$



Δ_2 at low Q^2



● Hall A ^3He data show $g_2 \approx -g_1$ for the neutron at low Q^2 .

● $g_1 + g_2 \propto \sigma_{LT}$ which should go to zero as $Q^2 \rightarrow 0$.

● $\beta_2(\tau) \rightarrow \frac{1}{4\tau}$ as $\tau \rightarrow \infty$ with

$\tau = \frac{Q^2}{4M^2x^2}$. Therefore, $\beta_2 = 0$ at

$x = 0$ and $\beta_2 = \frac{M^2Q^2}{(Q^2+m^2)^2}$ at x_{th} , with

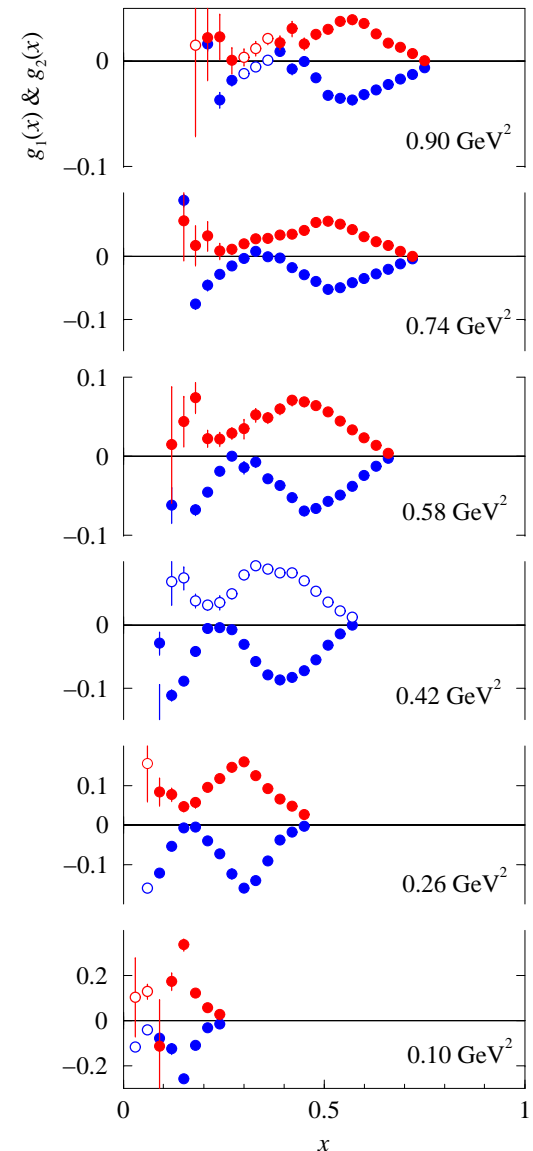
$$m^2 = m_\pi^2 + 2Mm_\pi$$

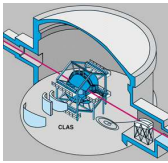
● Take average β_2 and $g_2 = -g_1$

$$\bullet \Delta_2^{[0,0.05]} =$$

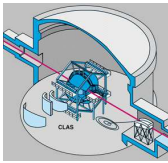
$$-24M^2 \int_0^{0.05} \frac{dQ^2}{Q^4} \frac{M^2Q^2}{2(Q^2+m^2)^2} \left(\frac{\kappa^2}{8M^2} Q^2 \right)$$

= -2.276 (numerically incorrect, but integral converges!)

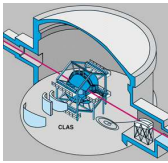




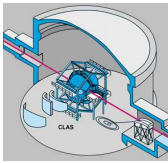
- $\langle r \rangle_Z = -\frac{4}{\pi} \int_0^\infty \frac{dQ}{Q^2} \left[G_E(Q^2) \frac{G_M(Q^2)}{1+\kappa} - 1 \right]$
- Unless G_E and G_M go as $1 + \epsilon Q^2$, the Zemach radius diverges.
- Bosted fit, PRC51(95)409:
 $G_E = 1/(1 + 0.14Q + 3.01Q^2 + 0.02Q^3 + 1.20Q^4 + 0.32Q^5)$
and $G_M = (1 + \kappa)G_E$ fits all data well; yet the Zemach integral diverges.
- JLab fit, ARNPS54(04)217,
 $(1 + \kappa)G_E/G_M = 1 - 0.13(Q^2 - 0.29)$ yields a divergent $\langle r \rangle_Z$.
- Friar and Sick's analysis assumes a convergent Q^2 dependence (reasonable); however, data alone are consistent with $\langle r \rangle_Z = \infty$.



term	Q^2 (GeV ²)	value	component
Δ_1	[0, 0.05]	-2.44 ± 1.2	
	[0.05, 20]	7.22 ± 0.72	F_2
		-1.10 ± 0.55	g_1
	[20, ∞]	0.00 ± 0.01	F_2
		0.12 ± 0.01	g_1
total		3.80 ± 1.5	
Δ_2	[0, 0.05]	-0.28 ± 0.28	
	[0.05, 20]	-0.33 ± 0.33	
	[20, ∞]	0.00 ± 0.01	
total		-0.61 ± 0.61	
Δ_{pol}		0.72 ± 0.37 ppm	



- Δ_{pol} is dominated by F_2 with a smaller (canceling) contribution from g_1 , and a small contribution from g_2 .
- Most of Δ_{pol} comes from $Q^2 < 1 \text{ GeV}^2$.
- Unless $F_2 \rightarrow \kappa + \epsilon Q^2$ and $\Gamma_1 = -\kappa^2 Q^2 / 8M^2$ (generalized GDH Sum Rule) as $Q^2 \rightarrow 0$, Δ_1, Δ_Z diverge.
- If $\Gamma_2 \rightarrow \kappa^2 Q^2 / 8M^2$ ($g_2 = -g_1$ and GDH) as $Q^2 \rightarrow 0$, Δ_2 converges.
- $\Delta_{\text{pol}} = 0.7 \pm 0.4$ ppm is small compared to $\Delta_{\text{pol}} = 3.3 \pm 0.6$ ppm from the HFS+Zemach analysis.
- Discrepancy most likely lies in the low- Q^2 dependencies of g_1, g_2, G_E and G_M .



- Determination of Δ_{pol} can be improved only by precision data for g_1 , g_2 and F_2 with $Q^2 < 1 \text{ GeV}^2$
- The behavior of g_1 , g_2 , and F_2 for $Q^2 < 0.05$ is crucial, since a large part of Δ_{pol} comes from this region.
- Although beautiful g_1 data exist from CLAS at JLab over a large kinematic region, the errors on this part are dominated by the lowest Q^2 data.
- Finite hyperfine splittings imply: $\Gamma_1 \rightarrow -\kappa^2 Q^2 / 8M^2$
 $g_2 \rightarrow -g_1$, $F_2 \rightarrow \kappa - \epsilon Q^2$, $G_E \rightarrow 1 - \epsilon_E Q^2$, and
 $G_M / (1 + \kappa) \rightarrow 1 - \epsilon_M Q^2$ as $Q^2 \rightarrow 0$.
- Higher orders (Q^4 , Q^6 , etc.) are crucial at low Q^2 for an accurate determination of Δ_{pol} .